Solid State Ionics 261 (2014) 17–20

Contents lists available at ScienceDirect

Solid State Ionics

journal homepage: www.elsevier.com/locate/ssi

Electronic structure and ionic diffusion of green battery cathode material: $Mg_2Mo_6S_8$

T. Kaewmaraya [a],*, M. Ramzan [a], J.M. Osorio-Guillén [b], R. Ahuja [a,c]

[a] Condensed Matter Theory Group, Department of Physics and Astronomy, Uppsala University, Box 516, SE-751 20 Uppsala, Sweden
[b] Instituto de Física, Universidad de Antioquia UdeA, Calle 70 No. 52-21, Medellín, Colombia
[c] Applied Materials Physics, Department of Materials Science and Engineering, Royal Institute of Technology, SE-100 44 Stockholm, Sweden

ARTICLE INFO

Article history:
Received 15 January 2014
Received in revised form 25 March 2014
Accepted 25 March 2014
Available online 18 April 2014

Keywords:
Mg-ion batteries
First-principle calculations
Hybrid functionals
Molecular dynamics

ABSTRACT

We report *ab-initio* density functional theory calculations of crystal and electronic structure of $Mg_2Mo_6S_8$, a candidate material to be used in rechargeable magnesium batteries, by employing hybrid exchange–correlation functionals. We find that $Mg_2Mo_6S_8$ crystalizes in a triclinic geometry and it is a semiconductor with an indirect band gap. *Ab-initio* molecular dynamics shows that Mg ions present progressive diffusion starting at 200 K with a preferable path through the channel between Mo_6S_8 blocks along the [010] direction. The intercalation voltage of the system is also determined and the results show that the voltage evaluated by PBE and hybrid functionals likely implies the lower and the upper limit of the experimental value. Lastly, we confirm the dynamical stability of the crystal structure by the calculated phonon dispersion relation.

1. Introduction

Increasing energy consumption in modern society has enormously stimulated the search for reliable, inexpensive and environmentally benign power sources. Nowadays, rechargeable lithium-ion (Li-ion) batteries are widely used for small-scale electronic applications such as mobile electronic gadgets. However, Li-ion batteries are not suitable for large-scale applications due to the limitations in safety and expensiveness [1], hindering them to surpass lead-acid batteries which are not eco-friendly. There have been a number of attempts to make rechargeable magnesium-ion (Mg-ion) batteries as an alternative because of several key benefits. Magnesium is comparatively more abundant and its divalent character is theoretically able to serve a higher volumetric energy density (3833 mA h cm^{-3}) than lithium (2061 mA h cm^{-3}) [2–4]. Magnesium metal anodes have been reported to deliver superior cycle life and efficiency [1]. Recent experiments [5] by using low-cost Sn as an anode material, Mo_6S_8 as a cathode material and conventional battery electrolyte ($Mg(N(SO_2CF_3)_2)_2$) have attained superior operating voltages and capacity for rechargeable Mg-ion batteries, strengthening the possibilities of Mg-ion batteries as large-scale energy supplies in the near future.

The cathode material, chevrel-type Mo_6S_8 is an appropriate host for numerous reasons. The presence of Mo_6 clusters can accommodate up to four electrons, suggesting remarkably high mobility of foreign multivalent cations inserted into Mo_6S_8 [6]. Mg atoms can be reversibly inserted/deinserted to form $Mg_xMo_6S_8$ ($0 \leq \times \leq 2$), yielding modifications in chemical and physical properties of the host material yet there are small disturbances in the crystal geometry [7,8]. In terms of ion mobility, it has been reported to depend on the concentration of Mg ions in the host material. Mg^{2+} ions diffuse in $MgMo_6S_8$ relatively slow due to their locations with low potential energy [7,8]. On the other hand, those in $Mg_2Mo_6S_8$ are considerably faster because of the stronger repulsion between Mg^{2+} cations, leading to a rapid diffusion through the material [7]. Crystal structures and ion diffusion mechanisms in $Mg_2Mo_6S_8$ have been experimentally revealed, but electronic properties, diffusion mechanisms, and structural stability from the theoretical point of view have been particularly limited [9]. Hence, detailed theoretical investigations of these issues are necessary.

2. Computational details

In the present study, we aim at theoretically investigating structural geometry, electronic properties, diffusion mechanism and structural stability of $Mg_2Mo_6S_8$ within the framework of the density functional theory (DFT). Total energy calculations were performed using the projector augmented-wave (PAW) method [10] as implemented in the VASP package [11,12]. We employed several *xc* functionals: Perdew–Burke–Ernzehof (PBE) [13], hybrid functional PBE0 [14], and screened hybrid functional of Heyd–Scuseria–Ernzerhof (HSE) [15]. We considered Mg ($2p^63s^2$), Mo ($4p^64d^55s^1$) and S ($3s^23p^4$) as valence

---

* Corresponding author at: Condensed Matter Theory Group, Department of Physics and Astronomy, Uppsala University, Box 516, SE-751, 20 Uppsala, Sweden.
E-mail address: thanayut.kaewmaraya@physics.uu.se (T. Kaewmaraya).

http://dx.doi.org/10.1016/j.ssi.2014.03.023
0167-2738/

electrons in potentials. A cut-off energy of 600 eV for the plane wave expansion incorporating with a 8 × 8 × 8 *k*-point grid for Brillouin-zone integrations was used throughout the calculations as the total energies of the unit cell were tested to ensure satisfactory convergence. Ionic coordinates, volume and shape of the crystal structures were simultaneously optimized until achieving the required accuracy i.e.; the Hellmann–Feynman forces exerting on each atom less than 0.001 eV/Å. For the determinations of density of states (DOS), a 12 × 12 × 12 *k*-point grid with the tetrahedron scheme for Brillouin-zone integrations was employed. In addition, we performed *ab-initio* molecular dynamic (AIMD) simulations to study diffusion of Mg ions in Mo_6S_8 by the following setting. The canonical ensemble with fixed volume *V*, temperature *T* and particle number *N* was considered. We carried out AIMD simulations at 200 K and 300 K for 15,000 time steps (time step of 1 fs). K-point mesh of 2 × 2 × 2 with the cut-off energy of 600 eV was applied. A supercell of 2 × 2 × 2 containing 128 atoms was used in the simulation. An assessment of structural stability was justified from phonon calculations based on a supercell approach. Atoms in the supercell were displaced from their equilibrium positions and forces acting on all the atoms were directly determined using VASP. These forces are subsequently collected to calculate phonon dispersions using the PHONOPY package [16].

3. Results and discussion

The crystal structure of $Mg_2Mo_6S_8$ is classified as a chevrel phase where a unit cell is made up of Mo_6S_8 blocks. Each block is composed of a cubic cage of eight sulfur atoms enclosing a distorted octahedral cluster of molybdenum atoms as depicted in Fig. 1(a). The Mg guest atoms usually occupy sites in the channels formed between these blocks and there are 12 possible lattice sites between every set of two blocks, six in the inner ring and other six in the outer ring as differently denoted by orange and light blue spheres in Fig. 1(b). However, maximal two Mg atoms per formula unit can be accommodated simultaneously because of electronic restrictions [17]. The representative primitive cell consisting of 16 atoms has been used to minimize computationally demanding hybrid functional calculations. We consider the atomic configuration that both Mg atoms are located at an outer ring as reported by ref. [1]. The optimized crystal parameters presented in Table 1 reveal a triclinic geometry of $Mg_2Mo_6S_8$, suggesting that the Mg insertions into Mo_6S_8 yield a triclinic structure at low temperature, in good agreement with previous theoretical study [9].

Table 1
Computed crystallographic parameters of $Mg_2Mo_6S_8$ crystal structures.

xc-Functional	*a* (Å)	*b* (Å)	*c* (Å)	α (deg)	β (deg)	γ (deg)
$Mg_2Mo_6S_8$						
PBE	6.634	6.702	6.596	90.86	97.95	99.37
HSE06	6.582	6.662	6.537	91.05	98.14	99.56
PBE0	6.581	6.663	6.536	91.06	98.12	99.57
PBE [9]	6.629	6.515	6.501	94.26	96.78	91.40

We have subsequently explored the electronic properties by calculating density of states (DOS) of Mo_6S_8 and $Mg_2Mo_6S_8$ as depicted in Fig. 2. PBE and HSE06 predict Mo_6S_8 to be metallic, characterized by states of dominant Mo-*4d* and S-*2p* at the Fermi level. We also employed PBE0 functional (not shown) and it also yields the metallic character. There is Mo-*4d*-S-*2p* hybridization at −6 to −2 eV (−8 to −2 eV for HSE06), which represents the covalent Mo–S bonding. The states above −2 eV are predominantly formed by Mo-*4d* and they account for Mo–Mo bonding and antibonding of Mo_6 clusters [18]. The predicted metallic character of Mo_6S_8 in this work is found to be consistent with the previous theoretical studies [9,19]. On the other hand, the presence of Mg atoms in Mo_6S_8 results in a metal–insulator transition as evidenced by DOS of $Mg_2Mo_6S_8$ in Fig. 2. The occupied states and unoccupied states are separated by an indirect gap of 1.1 eV (2.1 eV by HSE06). The observed difference in band gap calculated by PBE and HSE06 functionals is originated from the admixture of 25% Hartree–Fock exchange in HSE06, which relatively yields more spatial localization of Mo-*d* states as compared with conventional PBE [20]. The metal–insulator transition can be simply explained by band filling. The unoccupied states of Mo_6S_8 positioned around 1 eV above the Fermi level as shown in Fig. 2 are filled by donated electrons from Mg atoms, consequently yielding a gapless system. In addition, the right panel of Fig. 2 depicts a close-up of $Mg_2Mo_6S_8$ DOS near the band edges. There is a visible

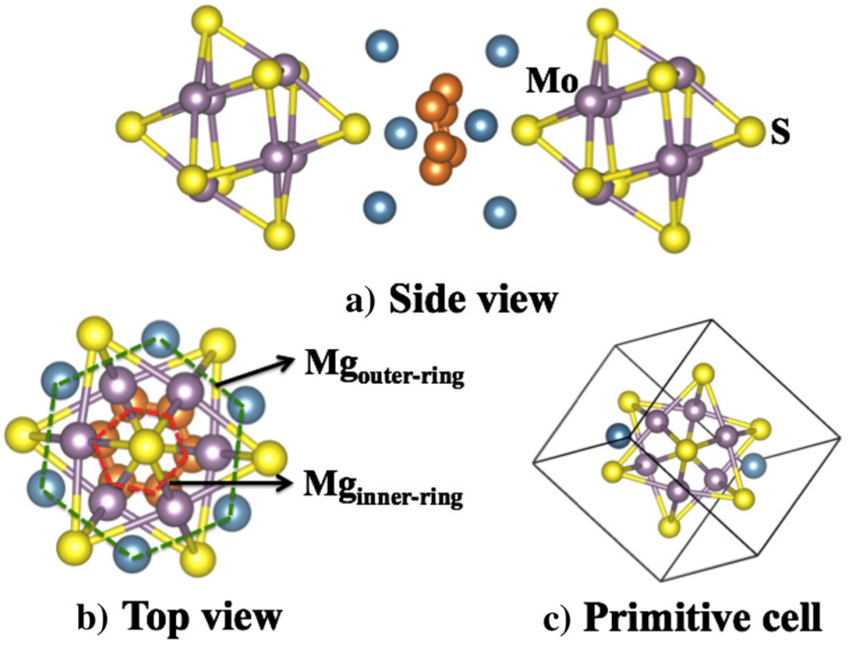

Fig. 1. Crystal structure: (a) side view and (b) top view of $Mo_xMo_6S_8$ (space group $R\overline{3}$) where Mg atoms can be accommodated between Mo_6S_8 cages, (c) the representative primitive cell employed in this study where 2 Mg atoms are located in the outer ring. Color coding is Mo (purple), S (yellow), Mg in the inner ring (orange) and Mg in the outer ring (blue).